Journal of Alloys and Compounds 504 (2010) 320–324

Contents lists available at ScienceDirect

Journal of Alloys and Compounds

journal homepage: www.elsevier.com/locate/jallcom

# High-temperature behaviour of Ti–Al–Si alloys produced by reactive sintering

Pavel Novák*, Filip Průša, Jan Šerák, Dalibor Vojtěch, Alena Michalcová

*Institute of Chemical Technology, Prague, Department of Metals and Corrosion Engineering, Technická 5, 166 28 Prague 6, Czech Republic*

ARTICLE INFO

*Article history:*
Received 19 April 2010
Received in revised form 14 May 2010
Accepted 21 May 2010
Available online 2 June 2010

*Keywords:*
Titanium aluminide
Titanium silicide
Reactive sintering
Powder metallurgy
Oxidation resistance
Thermal stability

ABSTRACT

Alloys formed by Ti–Al intermediary phases have low density and very good high-temperature oxidation resistance. Further improvement of high-temperature behaviour can be achieved by a suitable addition of silicon. In this work, Ti–Al–Si alloys containing 20 wt.% of aluminium and 10–20 wt.% of silicon produced by a reactive sintering technology were tested. Isothermal oxidation tests were carried out at 1000 °C in air. The oxidation rate was determined from weight gains caused by oxide formation. Microstructure and phase composition of the oxide layers were studied. Microstructure and hardness changes after various annealing durations were described.



## 1. Introduction

Bulk intermetallic phases from Ni–Al, Ti–Al and Fe–Al systems are promising high-temperature materials. These phases are advantageous for automotive or aerospace applications due to a good thermal stability and high-temperature oxidation resistance in combination with a density lower than common nickel- or iron-base heat resistant alloys. From this viewpoint, Ti–Al intermetallics have attracted high attention of both researchers and engineers. In this grade of materials, density decreases with growing aluminium content, while the high-temperature oxidation resistance and thermal stability increases. The application limits of $Ti_3Al$ phase are 760 °C in inert atmosphere (creep limit) and approx. 600 °C in air (oxidation limit) [1]. Application range of TiAl phase is higher—750 °C in air and approx. 900 °C in inert atmosphere or vacuum [1]. It shows that the temperature range of application of all Ti–Al phases is strongly limited by their high-temperature oxidation. To improve the high-temperature oxidation behaviour of these materials, additions of various alloying elements are applied. Positive effects of niobium and tantalum on high-temperature oxidation resistance were already described [2,3]. However these heavy elements undesirably increase the density and cost. Other possibility how to improve high-temperature behaviour is alloying with silicon. Titanium and silicon form stable $Ti_5Si_3$ silicide, which is used also in the surface treatment of titanium alloys against high-temperature oxidation [4,5].

Simple reactive sintering powder metallurgy production route for Ti–Al–Si alloys with aluminium content between 8 and 20 wt.% and silicon in the range of 10–20 wt.% was developed in our previous work [6,7] and room-temperature properties were described [6]. In this work, the oxidation resistance and thermal stability of these alloys are investigated at a temperature of 1000 °C, i.e. above the air operating limit for TiAl. Oxidation behaviour is compared with the TiAl binary phase produced by conventional vacuum melting technique.

## 2. Experimental

In this work, Ti–Al–Si alloys produced by reactive sintering of titanium, aluminium, silicon and AlSi30 powders were studied. Powders of titanium, aluminium and AlSi30 with a particle size of 200–600 μm were prepared by mechanical machining. Silicon powder with the particle size up to 50 μm was obtained by mechanical milling. Green bodies of Ti–Al–Si ternary alloys containing 20 wt.% of aluminium and 10–20 wt.% of silicon were produced by blending the above mentioned powders and uniaxial pressing at the laboratory temperature by a pressure of 260 MPa using Heckert FPZ100/1 universal loading machine. The green bodies had a cylindrical shape of 12 mm in diameter and 10 mm in height. Pressureless reactive sintering was carried out at a temperature of 900 °C for 30 min in an electric resistance furnace in evacuated and sealed silica ampoules. Heating rate of the sample to the reactive sintering temperature was approx. 300 K/min which was achieved by placing of the sample to the preheated furnace. Microstructure of prepared materials was observed by an Olympus PME3 light microscope and a Hitachi S-450 scanning electron microscope equipped with an EDS analyser. Hardness of the prepared materials was tested by the Vickers method with a load of 10 kg (HV 10). Silicide grain size was measured by the means of image analysis (LUCIA 4.8 image analysis software) as the equivalent diameter of a circle with the same area as the measured grain.

* Corresponding author.
*E-mail address:* panovak@vscht.cz (P. Novák).

0925-8388/$ – see front matter © 2010 Elsevier B.V. All rights reserved.
doi:10.1016/j.jallcom.2010.05.115

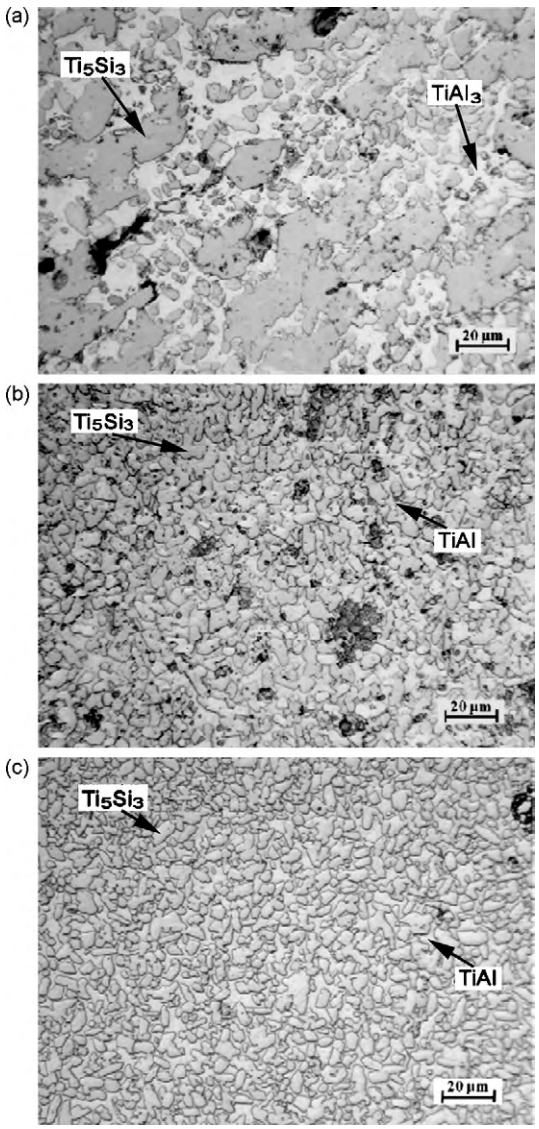


**Fig. 1.** Microstructure of (a) TiAl20Si20, (b) TiAl20Si15 and (c) TiAl20Si10 produced by reactive sintering at 900 °C for 30 min.

Isothermal oxidation tests were carried out at 1000 °C in air. Oxidation rate was determined from weight gains caused by the oxide formation on the surface of thermally exposed samples.

Microstructure of the oxide layers was documented by the light microscope, chemical and phase composition were determined by XRD (Philips X'Pert Pro X-ray diffractometer) and EDS. Raman spectroscopy (Horiba JobinYvon LABRAM HR Raman dispersion spectroscope with a spectral range of 100–4000 $cm^{-1}$) was also applied to identify the oxides. Thermal stability was studied by the hardness measurement (HV 10) and by the microstructure observation after long-term annealing at 1000 °C. For all of the above described tests, three samples of each alloy and conditions were used.

## 3. Results and discussion

### 3.1. Microstructure of the reactive sintering products

Fig. 1 shows the microstructure of the studied materials prepared by reactive sintering. Materials were prepared according to our previous experiments [7] to achieve the lowest possible porosity with the absence of residual non-reacted components. All alloys are formed by $Ti_5Si_3$ grains surrounded by titanium aluminide. TiAl20Si20 contains $TiAl_3$ phase (Fig. 1a). In the other materials, TiAl aluminide was determined (Fig. 1b and c). The average size of

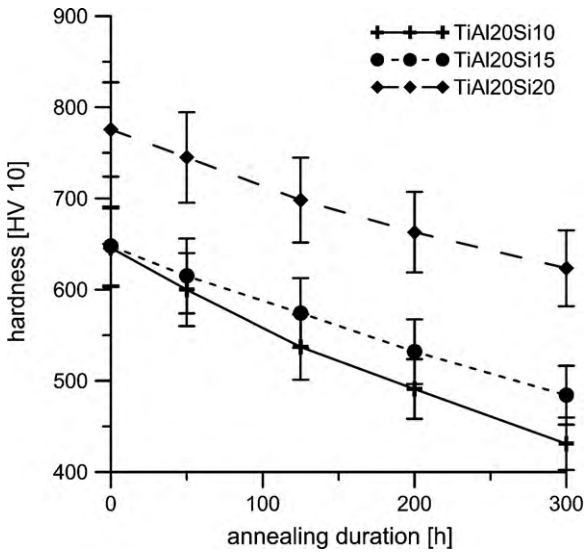


**Fig. 2.** Dependence of hardness of Ti–Al–Si alloys on duration of annealing at 1000 °C.

silicide grains reaches 6–7 μm in TiAl20Si10 and TiAl20Si15 alloys and approx. 12 μm in the alloy with 20 wt.% of silicon. Porosity of all the investigated alloys is below 10 vol.% and is concentrated mainly in the centre of the sample as it was described in Ref. [6]. The mechanism of formation of the porosity proposed in Ref. [6] is following: during the heating in the electric resistance furnace, the reaction starts on the surface and propagates to the core of the green body. The material is probably locally melted by the heat evolved during the reaction. Residual pores and gas trapped inside during pressing remain in the centre of the product.

### 3.2. Thermal stability

During annealing of the investigated alloys at 1000 °C, gradual hardness decrease can be observed. Softening during annealing strongly depends on the alloy composition (Fig. 2). The smallest hardness changes with the annealing time were detected in alloys containing 15–20 wt.% of silicon.

As it is evident by comparing the microstructure before (Fig. 1b) and after annealing (Fig. 3), the hardness decrease is caused by coarsening of $Ti_5Si_3$ grains. In the case of TiAl20Si10 alloy, annealing at 1000 °C for 300 h induced an increase of the average silicide grain size from approx. 6 μm to more than 13 μm. The dependence of the silicide grain size on annealing time is linear in all investi-

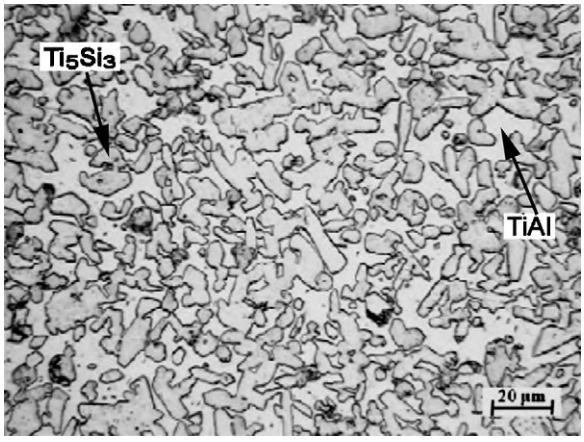


**Fig. 3.** Microstructure of TiAl20Si15 alloy after annealing at 1000 °C for 300 h.

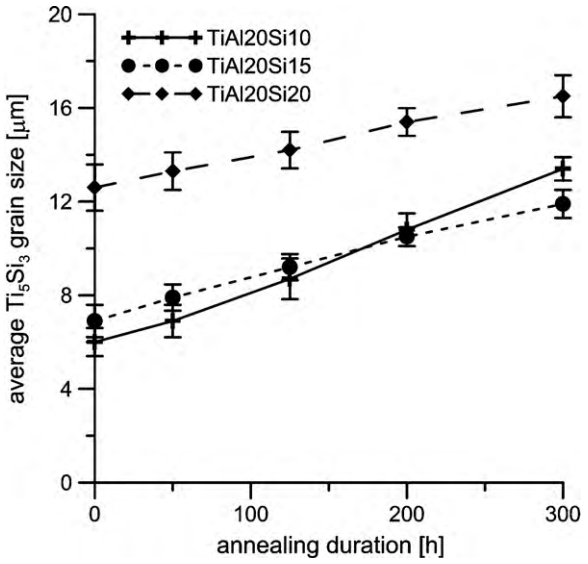


**Fig. 4.** Average equivalent diameter of $Ti_5Si_3$ grains vs. duration of annealing at 1000 °C.

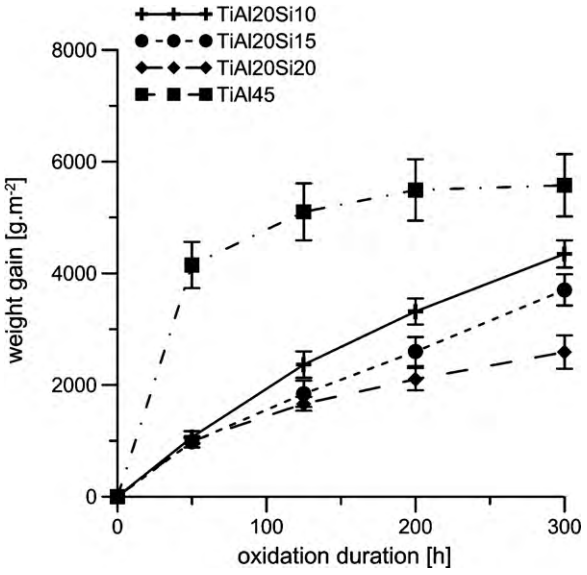


**Fig. 5.** Dependence of specific weight gain [g m$^{-2}$] on duration of oxidation at 1000 °C in air.

gated alloys (Fig. 4) and can be described by an empiric equation according to the grain growth kinetics published in [8]:

$$d(Ti_5Si_3) - d_0(Ti_5Si_3) = A \cdot t, \quad (1)$$

where $d(Ti_5Si_3)$ is the average equivalent diameter of silicide grains [μm], $t$ represents annealing time [h] and $A$ and $d_0(Ti_5Si_3)$ are the coarsening rate [μm h$^{-1}$] and the initial silicide grain size [μm], respectively.

In TiAl20Si20 alloy exhibiting the lowest hardness decrease, the coarsening rate of silicide (constant A) is significantly lower than that of TiAl20Si10 and TiAl20Si15 alloys. It shows that the hardness decrease is proportional to the silicide coarsening rate (Table 1).

### 3.3. High-temperature oxidation

The oxidation tests at 1000 °C showed, that the oxidation rate strongly depends on the silicon content (Fig. 5). The higher is the silicon content, the lower is the weight gain caused by oxide formation. The highest weight gains were determined in the case of cast TiAl45 alloy which was applied as a reference material in oxidation test.

Process controlling the oxidation was determined by fitting the layer thickness, calculated from the weight gains, by the linear or parabolic growth equation. Linear growth mode can be usually found during short reaction times. This so-called linear law is described by Eq. (2) [9,10]:

$$d = K(t - \tau), \quad (2)$$

where $d$ is the layer thickness, $K$ is the linear rate constant, $t$ and $\tau$ are the reaction time and incubation period, respectively. When the layer growth obeys the linear law, the process is controlled by the rate of chemical reaction producing the intermetallics layer [9,10].

When a process is controlled by diffusion of species through a reaction product, it is generally described by the parabolic law, written as:

$$d^2 = 2 \cdot D \cdot t, \quad (3)$$

where $D$ is the diffusion coefficient of the most slowly diffusing element forming the layer [9,11,12].

Assuming that oxygen diffusion through the oxide layer is a common process controlling the oxidation, apparent diffusion coefficients of oxygen were calculated by Eq. (3), see Table 2. The apparent diffusion coefficients are almost constant with oxidation

**Table 1**
Kinetic parameters of silicide coarsening.

| Alloy | $A$ (μm h$^{-1}$) | $d_0$ ($Ti_5Si_3$) (μm) |
|---|---|---|
| TiAl20Si10 | 0.025 | 5.8 |
| TiAl20Si15 | 0.017 | 7.0 |
| TiAl20Si20 | 0.013 | 12.6 |

**Table 2**
Apparent diffusion coefficients [$\times 10^{-12}$ m$^2$ s$^{-1}$] of oxygen in oxide layers on Ti–Al–Si alloys at 1000 °C.

| Time (h) | TiAl20Si10 | TiAl20Si15 | TiAl20Si20 |
|---|---|---|---|
| 50 | 1.21 | 1.02 | 1.06 |
| 125 | 2.38 | 1.44 | 1.18 |
| 200 | 2.93 | 1.79 | 1.18 |
| 300 | 3.35 | 2.43 | 1.19 |

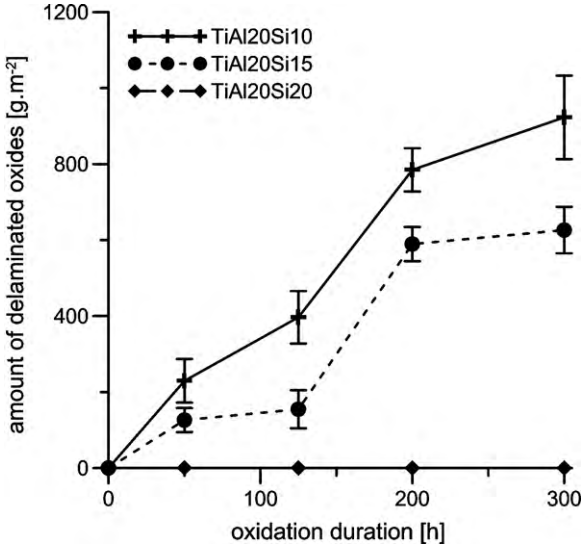


**Fig. 6.** Weight of delaminated oxides vs. duration of oxidation.

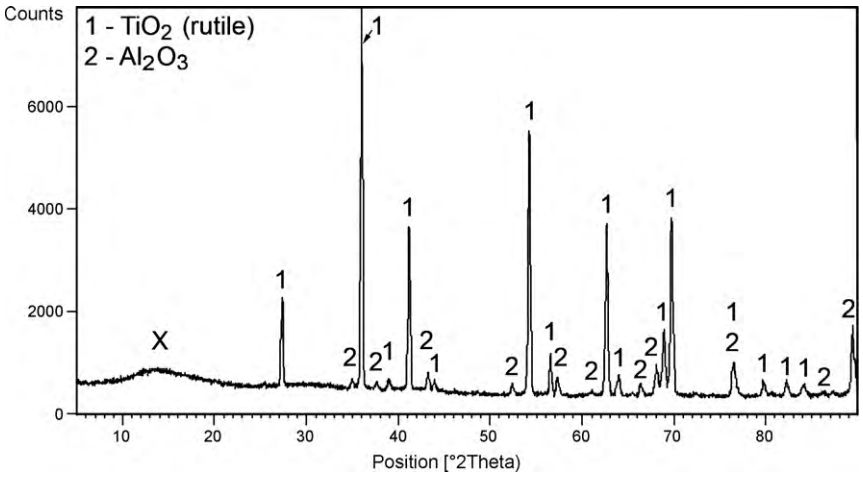


**Fig. 7.** XRD pattern of TiAl20Si15 alloy after oxidation at 1000 °C for 300 h.

time in the case of TiAl20Si20 alloy. It indicates that this process is controlled by the inward oxygen diffusion. In the other investigated alloys the apparent diffusion coefficients continuously increase with the oxidation duration. This behaviour can be explained by a delamination of oxide layers that renew the fresh surface for further oxidation. Another explanation can be a high porosity of the oxidation products. In alloys containing 10–15 wt.% of silicon, both of these features were identified. The amount of scaled oxides vs. oxidation duration and alloy composition is plotted in Fig. 6. Massive oxide delamination (120–930 g $m^{-2}$) was observed in the case of TiAl20Si10 and TiAl20Si15, while the TiAl20Si20 alloy exhibited a good adherence of oxidized layer to the metallic substrate.

XRD revealed the presence of corundum ($Al_2O_3$) and rutile ($TiO_2$) in the oxidized layer (Fig. 7). In addition to these two phases, an amorphous peak (marked "X") can be seen in the XRD pattern in Fig. 7, probably belonging to some amorphous silicon-containing phase. Presence of such phase was also recognized by EDS analysis, which showed silicon-rich regions in the oxide layer. Raman spectroscopy carried out on the outer surface of the oxide layer revealed only rutile ($TiO_2$), see Fig. 8. Other modifications of titanium dioxide (anatase, brookite) were not identified since these ones are formed at lower oxidation temperatures [13].

Microstructure of layers formed by oxidation at 1000 °C in air consists of one or two sub-layers, see Fig. 9. Oxide layers on alloys containing 10–15 wt.% of silicon are composed of two sub-layers (Fig. 9a). On the surface, $TiO_2$-rich layer (I.) with low content of $Al_2O_3$ can be recognized, as proved by chemical and phase analysis. Second sub-layer (II.) beneath the previous one is composed of $TiO_2$, $Al_2O_3$ and an amorphous silicon-containing compound marked by "X" in XRD pattern in Fig. 7. This sub-layer is also enriched by nitrogen, probably in the form of a nitride. In these alloys, oxide layers are porous and their adherence to the basic material is poor. On the other hand, the alloy containing 20 wt.%

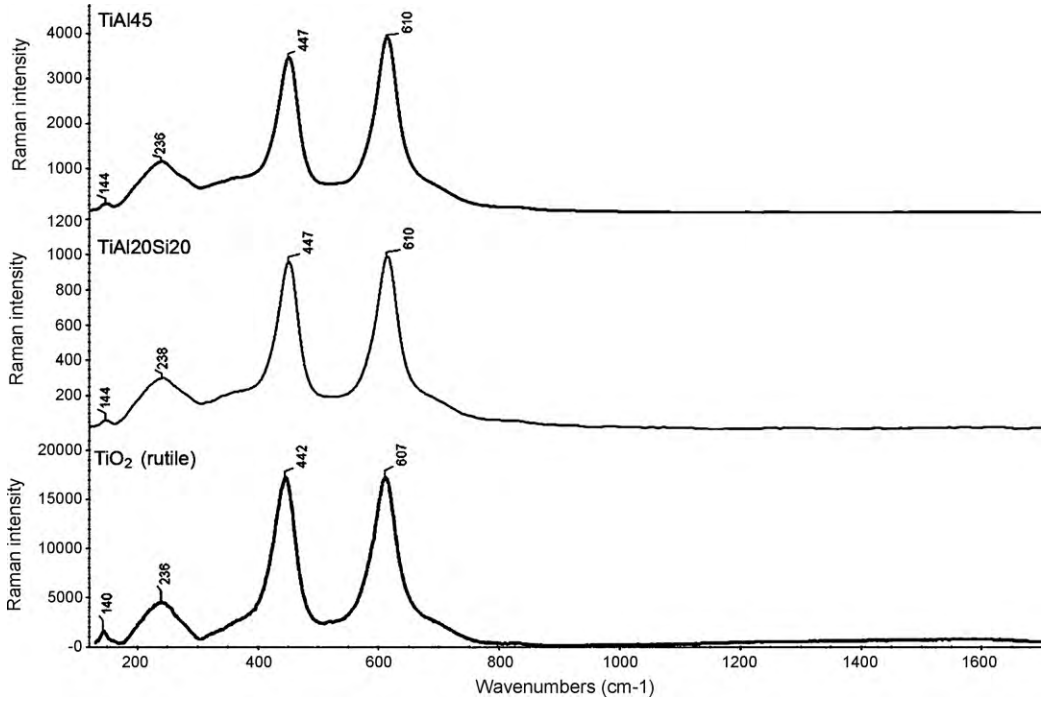


**Fig. 8.** Raman spectra of TiAl45 and TiAl20Si20 samples oxidized at 1000 °C compared with rutile spectrum.

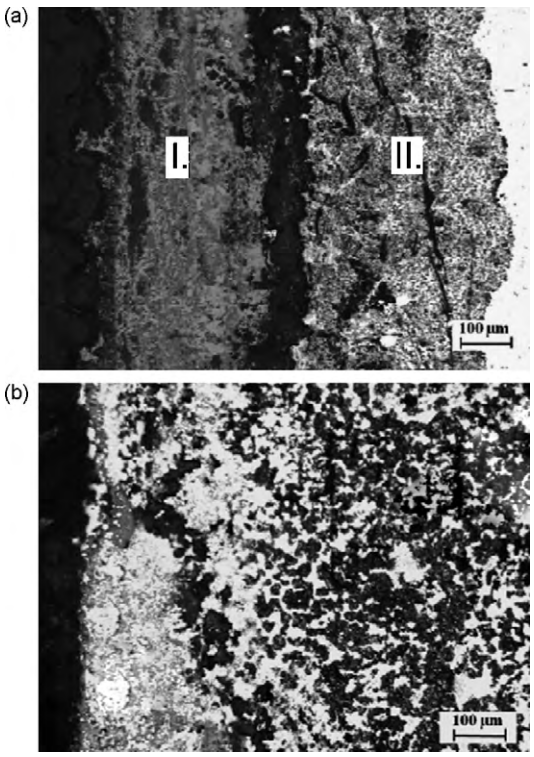


**Fig. 9.** Microstructure of the oxide layers on (a) TiAl20Si10 and (b) TiAl20Si20 alloys after oxidation at 1000 °C for 300 h.

of silicon forms only one compact oxide layer consisting of $TiO_2$, $Al_2O_3$ and a silicon-containing compound with good adherence to the substrate (Fig. 9b). The superior oxidation resistance is probably caused by two factors: high content of silicon in the alloy and the matrix formed by $TiAl_3$ phase which was published to have superior oxidation resistance to TiAl phase [14,15].

## 4. Conclusion

In this work, the oxidation resistance and thermal stability of Ti–Al–Si alloys produced by reactive sintering were studied at 1000 °C. Structure of the investigated materials is formed by $Ti_5Si_3$ and TiAl or $TiAl_3$. During annealing, hardness of these alloys decreases due to a coarsening of silicides. The lowest hardness decrease was determined for the alloy containing 20 wt.% of silicon. This material also exhibits exceptional high-temperature oxidation resistance without any delamination of the oxide layers.

## Acknowledgement

This work was financially supported by KJB201250801 research project of Grant Agency of AS CR and by the MSM 6046137302 research project of the Ministry of Education, Youth and Sport of the Czech Republic.

## References

[1] A. Lasalmonie, Intermetallics 14 (2006) 1123–1129.
[2] X. Lu, E. He, Journal of Alloys and Compounds 478 (2009) 220–225.
[3] T. Izumi, T. Yoshioka, Intermetallics 13 (2005) 694–703.
[4] D. Vojtěch, et al., Intermetallics 14 (2006) 1181–1186.
[5] D. Vojtěch, et al., Journal of Alloys and Compounds 464 (2008) 179–184.
[6] P. Novák, et al., Journal of Alloys and Compounds 470 (2009) 123–126.
[7] P. Novák, T. Popela, J. Kubásek, J. Šerák, D. Vojtěch, A. Michalcová, Powder Metallurgy (2009), doi:10.1179/174329009X409651.
[8] J. Reis, R. Chaima, Materials Science and Engineering A 491 (2008) 356–363.
[9] P. Novák, J. Kubásek, J. Šerák, D. Vojtěch, A. Michalcová, International Journal of Materials Research 100 (2009) 3.
[10] N. Birks, Introduction to the High Temperature Oxidation of Metals, second edition, Cambridge University Press, 2006.
[11] P. Novák, D. Vojtěch, J. Šerák, M. Novák, B. Bártová, Defect and Diffusion Forum 263 (2007) 87–92.
[12] P. Novák, V. Knotek, M. Voděrová, J. Kubásek, J. Šerák, A. Michalcová, D. Vojtěch, Journal of Alloys and Compounds (2010), doi:10.1016/j.jallcom.2010.03.028.
[13] http://en.wikipedia.org/wiki/Anatase.
[14] J.L. Smialek, Corrosion Science 35 (1993) 1199–1208.
[15] K. Hirukawa, H. Mabuchi, Y. Nakayama, Scipta Metallurgica et Materialia 25 (1991) 1211–1216.